Volume 17, Number 5, 2023. pp. 545-556

Jordan Journal of Physics

ARTICLE

Structural, Optical, Elemental and Thermal Characteristics of Pure and Magnesium Sulfate-Doped Growth Thiourea Crystals

D. Priya Dharshini[a], **C. Hentry**[b] and **B. Leema Rose**[b]

[a] *Research Scholar (Reg.no: 19213232132011), Department of Physics, St. Jude's College, Thoothoor, Affiliated to Manonmaniam Sundaranar University, Abishekapatti, Tirunelveli, 627012, Tamilnadu, India.*
[b] *Department of Physics, St. Jude's College, Thoothoor, 629176, Tamilnadu, India.*

Doi: **https://doi.org/10.47011/17.5.3**
Received on: 06/03/2023; *Accepted on: 18/07/2023*

Abstract: The growth of single crystals of pure and magnesium sulfate ($MgSO_4$)-doped Thiourea (TU) was accomplished through solvent evaporation. The crystals were characterized using X-ray powder diffraction, FTIR, EDAX, UV-visible, and TG/DTA techniques. The $MgSO_4$-doped TU crystal exhibited excellent optical transmission across the entire visible range. The metal complexes of TU enhanced the lower cut-off wavelength by 14.85 nm compared to pure TU, which is an essential requirement for a nonlinear optical material.

Keywords: Optical material, Magnesium sulfate, Gravimetric, Structural resemblance, Thiourea.

1. Introduction

Low-temperature solution growth is the simplest and, in many cases, the least expensive method for the production of optical crystals. Nonlinear optical materials (NLO) have a number of applications, such as second harmonic generation, frequency mixing, electrooptic modulation, etc. Organic NLO materials have garnered significant interest for their potential use in optical devices because of their large optical nonlinearity, low cut-off wavelength, short response time, and high laser damage threshold [1]. TU belongs to a class of organic compounds containing sulfur, with the general formula $(R_1R_2N)(R_3R_4N)C{=}S$. TU shares a structural resemblance with urea, except the oxygen atom in urea is replaced by a sulfur atom in TU. However, the chemical properties of urea and TU differ significantly [2]. TU derivatives are also widely utilized in drug design and medicinal chemistry. Figures 1(a) and 1(b) depict the chemical structures of TU and urea, respectively.

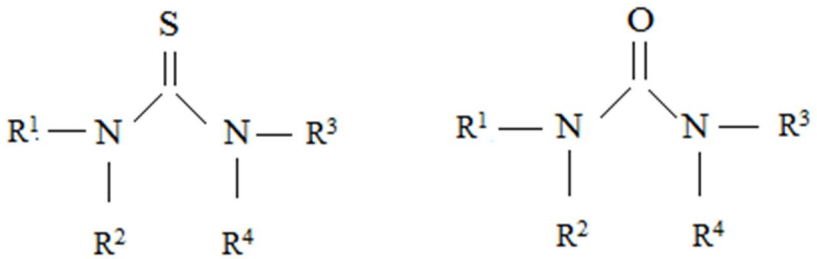

FIG. 1. (a) Thiourea and (b) Urea.

Corresponding Author: D. Priya Dharshini **Email**: priyadhason97@gmail.com

TU is an interesting inorganic matrix modifier, and it has the ability to form an extensive network of hydrogen bonds [3]. TU inorganic metal complex crystals with interesting optical, crystalline perfection, dielectric, mechanical, and electronic properties, as evidenced by investigators, are bis(TU) cadmium chloride, bis(TU) zinc chloride, bis(TU) cadmium acetate, bis(TU) cadmium acetate [4, 5], etc. The molecular structure of TU has been investigated using C2 symmetry constraints [6].

Organic ligands and small-electron systems, such as TU, thiocyanate, and urea, have been used with remarkable success. The centrosymmetric TU molecule, when combined with an inorganic salt, yields non-centrosymmetric complexes, which have NLO properties [7]. TU crystals also exhibit a pyroelectric effect, which is utilized in infrared (IR), ultraviolet (UV), scanning electron microscopy (SEM), and infrared imaging [8]. TU is one of the few simple organic compounds with high crystallographic symmetry. It crystallizes in the rhombic pyramidal division of the rhombic system and acts as a good ligand [9]. TU forms a number of NLO-active metal coordination compounds [10-14].

In the present investigation, pure and $MgSO_4$-doped TU crystals with various mole percentages were grown using the solvent evaporation technique.

2. Experimental

2.1. Materials

All the reagents used in the present study were of analytical grade. Thiourea (99%) was purchased from Merck. The solvent used in all the experiments was double-distilled water.

2.2. Temperature Dependence on Solubility

The maximum amount of a solute that dissolves in a known quantity of solvent at a certain temperature is its solubility. Temperature affects solubility. In the present investigation, the solubility of TU and $MgSO_4$-doped TU in double-distilled water was estimated at various temperatures ranging from 25ºC to 50ºC, in steps of 5ºC, using the gravimetric method. The results are presented in Table 1.

TABLE 1. Solubility of TU and $MgSO_4$-doped TU in double-distilled water.

Temperature (ºC)	Solubility pure TU g/L	Solubility $MgSO_4$-doped TU
25	141.5	145.4
30	163.9	167.1
35	190.5	194.4
40	234.5	238.2
45	280.2	284.1
50	414.9	418.3

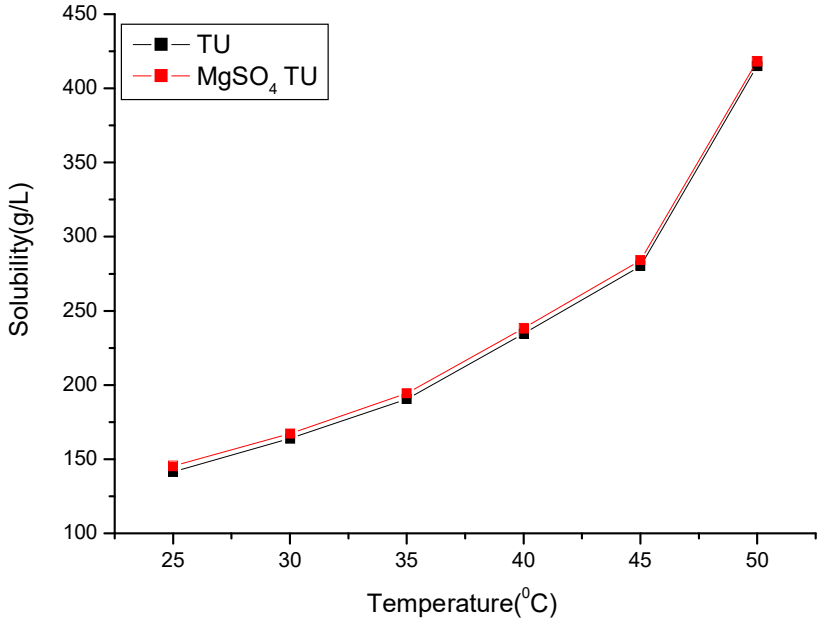

FIG. 2. Solubility curve of TU and $MgSO_4$-doped TU.

The collected data shows that the solubility of TU increases with an increase in temperature; the addition of $MgSO_4$ to the pure TU solution increases the solubility and has a positive temperature coefficient of solubility.

2.3. Crystal growth

A 350 ml of saturated solution of TU was dissolved in double-distilled water using a magnetic stirrer at a constant rate for 6 hours at a temperature of 30 ºC. After attaining saturation, the solution was filtered using Whatman filter paper with a pore size of 11.5 mm. A clean and dry 250 ml beaker was used in the present investigation. 50 ml of the saturated solution was taken from seven such beakers. One beaker was left as the standard for pure TU solution. In all the other beakers, the solution was doped with 0.1 M%, O.2 M%, 0.3 M%, 0.4 M%, 0.5 M%, and 0.6 M% of magnesium sulfate. All crystallizers were covered with perforated polythene paper and placed on a vibration-free platform. After 21 days, fully matured crystals of pure TU and $MgSO_4$-doped TU were obtained. Figure 3 illustrates the grown crystals: Fig. 3(a) shows the crystal of pure TU; Figs. 3(b), 3(c), and 3(d) show the $MgSO_4$ lightly doped TU crystals; Figs. 3(e), 3(f), and 3(g) show the heavily doped MgSO4 TU crystals. The morphology of the TU crystals changed as the concentration of the dopant increased.

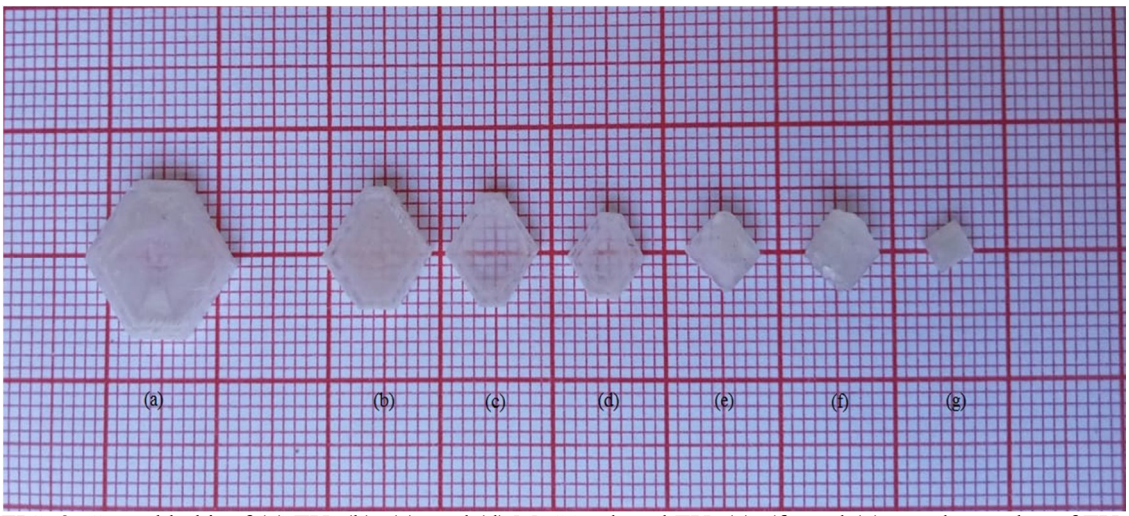

FIG. 3. Crystal habit of (a) TU; (b), (c), and (d) $MgSO_4$-doped TU; (e), (f), and (g) metal complex of TU.

2.4. Characterization

The structural analysis is represented by the details from the X-ray diffractometer (P-Analytical X-Pert-Pro-Diffractometer system with cuKα (Kα = 1.54060 ºA) radiation 2θ range at 10˚ - 90˚). The optical studies were performed using Fourier transform infrared spectroscopy (FTIR-Perkin Elmer wavelength range of 4500 cm^{-1} to 500 cm^{-1}). Micro-morphological studies were conducted using energy-dispersive X-ray analysis (EDXA) with a BRUKER system. We used a UV-visible spectrophotometer (Perkin Elmer Lambda-35 UV-Vis range at 200-800 nm). Thermal analysis studies were carried out using thermal gravimetric and differential thermal analysis (TGA/DTA, NETZSCH STA 2500 at a heating rate of 20°C/min in the temperature range of 30°C - 500°C).

3. Results and Discussion

3.1. Structural Analysis

The powder XRD patterns of pure TU, $MgSO_4$-doped TU, and metal complexes of $MgSO_4$-doped TU crystals are shown in Figs. 4. (a), 4(b), and 4(c), respectively.

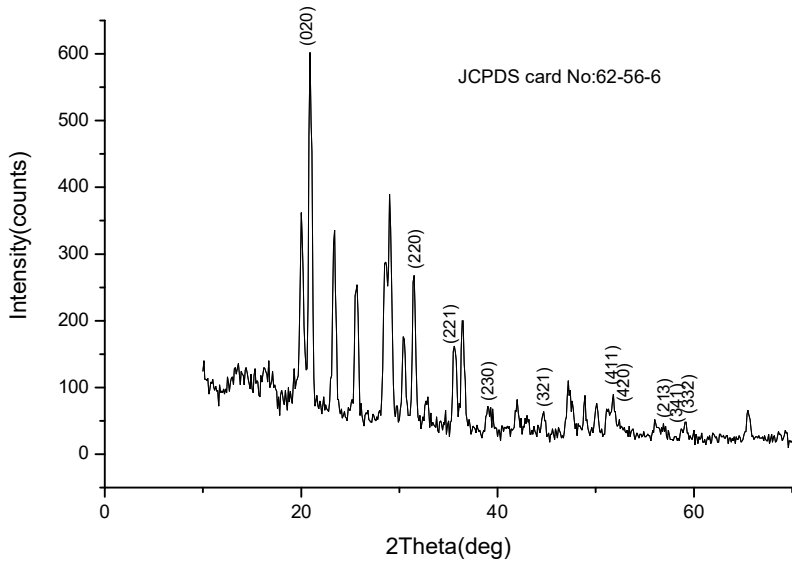

FIG. 4(a) XRD spectrum of pure TU.

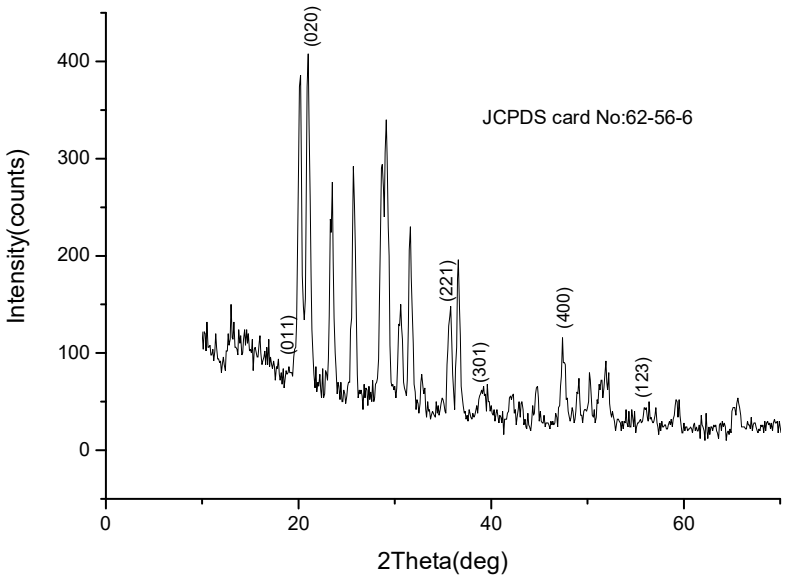

FIG. 4(b) XRD spectrum of $MgSO_4$-doped TU.

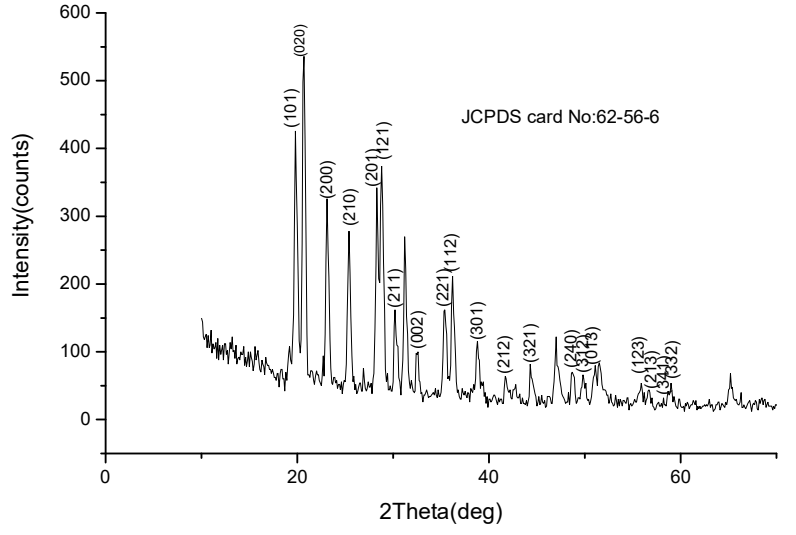

FIG. 4(c) XRD spectrum of metal complexes of $MgSO_4$-doped TU.

TABLE 2. Cell parameters of $MgSO_4$-doped TU and its metal complex.

Cell parameters (Aº)	JCPDS value of TU (Aº)	Reference value of TU (Aº) [15]	Calculated value of TU (Aº)	$MgSO_4$-doped TU (Aº)	Metal complexes of TU (Aº)
a	7.664	7.644	7.646	7.661	7.677
b	8.559	8.527	8.564	8.415	8.539
c	5.492	5.493	5.474	5.512	5.498
Cell volume (A^3)	360.31	358.04	358.45	355.32	360.41

The powder XRD pattern reveals an orthorhombic crystal system. The space group of pure and $MgSO_4$-doped TU crystals was Pnma 62. Figure 4(a) shows the sharp peaks of pure crystal, revealing the crystallinity of grown crystals. The observed peaks in the powder XRD pattern were properly indexed, and the cell parameters were calculated using unit cell software. The results for the pure crystal are: a = 7.646 Å, b = 8.564 Å, and c = 5.474 Å, with a calculated cell volume of 358.45 Å³.

Figure 4(b) depicts the sharp peaks of the MgSO4-doped TU crystals, which also exhibit excellent crystallinity. The calculated cell parameters for these crystals are: a = 7.661 Å, b = 8.415 Å, and c = 5.512 Å, resulting in a cell volume of 355.32 Å³.

Figure 4(c) shows the XRD pattern of the MgSO4-doped TU metal complex crystals, also revealing their crystallinity. The cell parameters were determined as a = 7.677 Å, b = 8.539 Å, and c = 5.498 Å, with a calculated cell volume of 360.41 Å³.

The observed XRD patterns are consistent with the standard JCPDS card No. 62-56-6 and previously reported values. Minor variations in the unit cell parameters of the MgSO4-doped TU crystals were noted, which may be attributed to the incorporation of magnesium ions into the crystal lattice.

3.2. Vibrational Analysis

The FTIR spectra of pure TU, $MgSO_4$-doped TU, and metal complexes of TU are presented in Figs. 5 (a), (b), and (c), respectively.

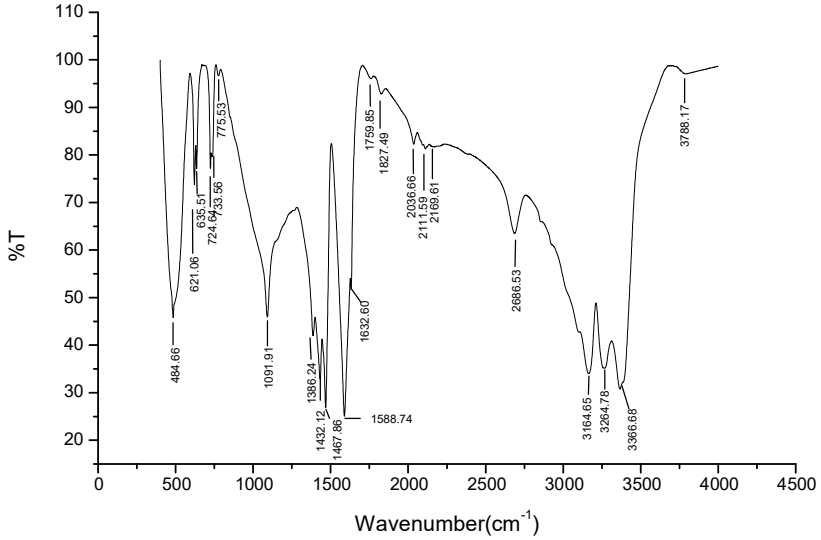

FIG. 5(a) FTIR spectrum of pure TU.

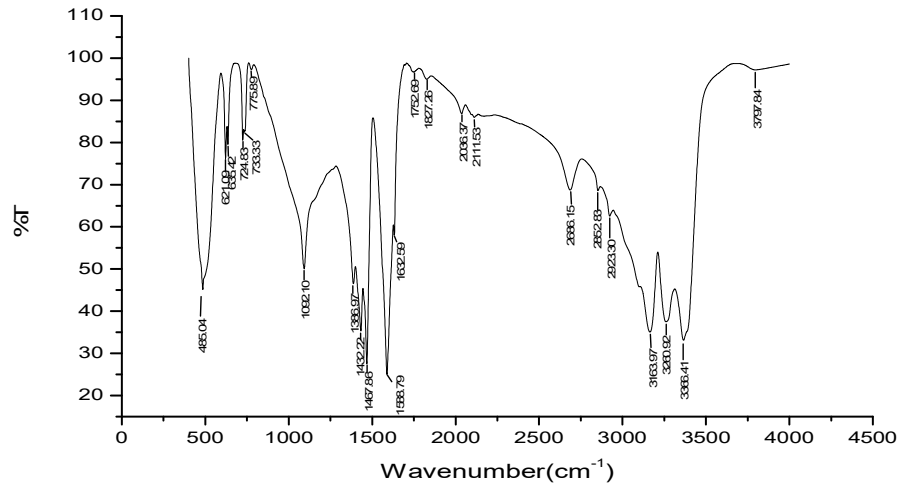

FIG. 5(b) FTIR spectrum of $MgSO_4$-doped TU.

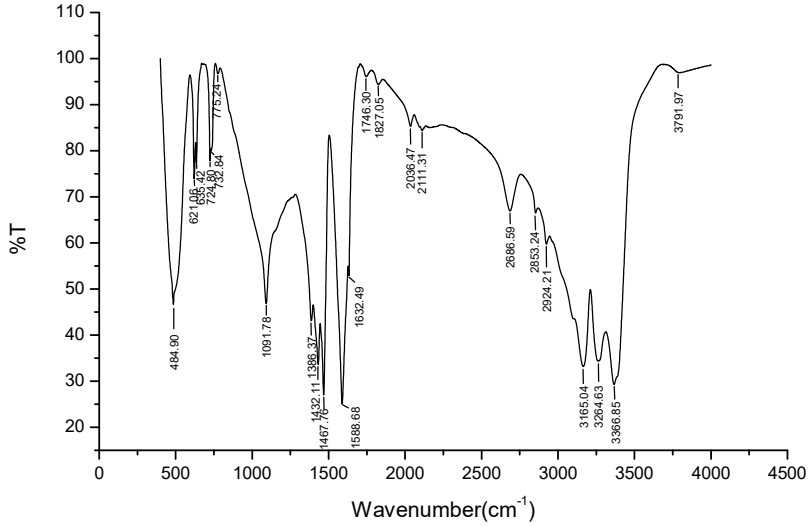

FIG. 5(c) FTIR spectrum of metal complex of $MgSO_4$-doped TU.

TABLE 3. Wave number assignments for pure and $MgSO_4$-doped TU and the metal complex of $MgSO_4$-doped TU in cm^{-1}.

Pure TU	$MgSO_4$-doped TU	Metal complex of $MgSO_4$-doped TU	Spectral Assignment
484.66	485.04	484.90	C-N-C Bending
621.06	621.09	621.06	S-O Stretching
635.51	635.42	635.42	SO_4 Bends
724.67	724.84	724.80	CH_2 Rocking vibration
733.56 and 775.53	733.56 and 775.53	732.80 and 775.24	Aromatic out of plane C-H Stretching
1091.91	1092.10	1091.78	C-O-C Asymmetric Stretching
1386.24	1386.97	1386.37	C=S Asymmetric Stretching
1432.12	1432.22	1432.11	C-N Stretching
1467.86	1467.86	1467.76	C=S Stretching
1588.74	1588.79	1588.68	N-S Scissoring
1632.60	1632.59	1632.49	N-H Bending
1759.85 and 1827.49	1752.69 and 1827.26	1746.30 and 1827.05	Symmetric C=O Stretching
2036.66	2036.66	2036.47	CH_2 rocking
2111.59	2111.59	2111.31	C≡C Stretching
2169.61	-	-	C≡C Stretching
2300-3500	2300-3500	2300-3500	NH & CH Stretching vibration
3788.17	3788.17	3791.97	O-H and C-H Stretching

The FTIR spectra of the pure and $MgSO_4$-doped TU crystals are represented in Figs. 5(a), 5(b), and 5(c). The spectra of the pure TU are assigned to the C-N-C bending characteristic form present at peak 484.66 cm^{-1}[16], S-O stretching characteristic form present at peak 621.06 cm^{-1}, SO_4 bending characteristic form present at peak 635.51 cm^{-1}, CH_2 rocking vibration characteristic form present at peak 724.67 cm^{-1}, aromatic out-of-plane C-H stretching form is present at peaks of 733.56 cm^{-1} and 775.53 cm^{-1}, C-O-C asymmetric stretching characteristic form present at peak 1091.91 cm^{-1}, C=S asymmetric stretching characteristics are present at peak 1386.24 cm^{-1}[17]. C-N stretching characteristic form is present at peak 1432.12 cm^{-1}, C=S stretching characteristic form is present at peak 1467.86 cm^{-1}, N-S scissoring characteristic form is present at peak 1588.74 cm^{-1}, N-H bending characteristic form is present at peak 1632.60 cm^{-1}. Symmetric C=O stretching characteristic form is present at peaks 1759.85 cm^{-1} and 1827.49 cm1. Additionally, CH_2 rocking is detected at 2036 cm^{-1}, while C≡C stretching occurs at 2111.59 cm^{-1} and C=C stretching is seen at 2169.61 cm^{-1} [20]. The N–H and C–H stretching bands are observed between 2300–3500 cm^{-1}, and O–H and C–H stretching are seen at 3788.17 cm^{-1} [19]. Of particular note is the absence of the peak at 2169.61 cm^{-1} (C=C stretching) in the MgSO4-doped TU and metal complex crystals, which suggests the incorporation of MgSO4 into the TU crystal structure. The FTIR spectral assignments for pure TU, MgSO4-doped TU, and their metal complexes are displayed in Figs. 5(a), 5(b), and 5(c).

3.3. EDAX Analysis

Energy dispersive X-ray (EDAX) analysis was performed to identify the elements present in the pure and $MgSO_4$-doped TU crystals, as well as their metal complexes, and to determine the atomic weight percentages of these elements. The elemental analysis revealed the presence of carbon, nitrogen, sulfur, magnesium, copper, potassium, iron, and sodium, confirming that the samples consisted of pure TU, $MgSO_4$-doped TU, and their metal complexes.

When comparing the elemental data for pure TU, $MgSO_4$-doped TU, and the metal complexes, copper, potassium, iron, and sodium were found exclusively in the metal complexes of $MgSO_4$-doped TU. Magnesium was present in both the $MgSO_4$-doped TU and its metal complexes. The atomic weight and weight percentages of magnesium were higher in $MgSO_4$-doped TU compared to the metal complex. Additionally, the atomic weight and weight percentages of carbon and nitrogen increased in $MgSO_4$-doped TU, while these values decreased in the metal complexes. The atomic weight and weight percentages of sulfur decreased in $MgSO_4$-doped TU but increased in the metal complexes. These changes can be attributed to the incorporation of $MgSO_4$ into the TU crystal structure and its metal complexes.

It should be noted that EDAX analysis does not detect hydrogen, which is why hydrogen was not included in the elemental data for pure and $MgSO_4$-doped TU or their metal complexes, as shown in Table 4 and Figs. 6(a), 6(b), and 6(c).

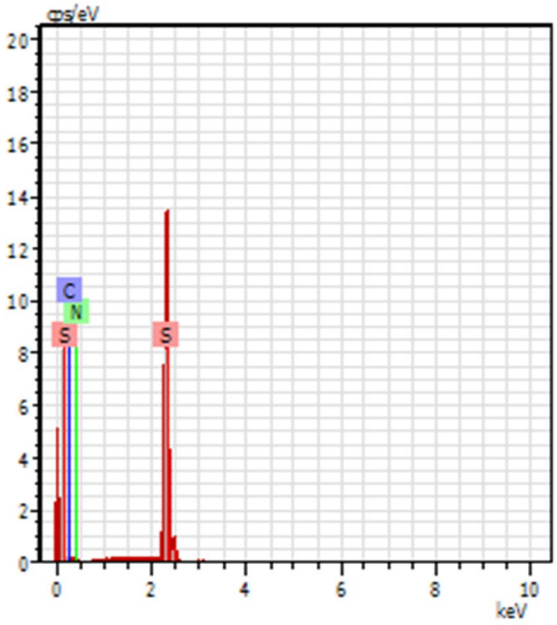

FIG. 6(a) EDAX spectrum of pure TU crystal

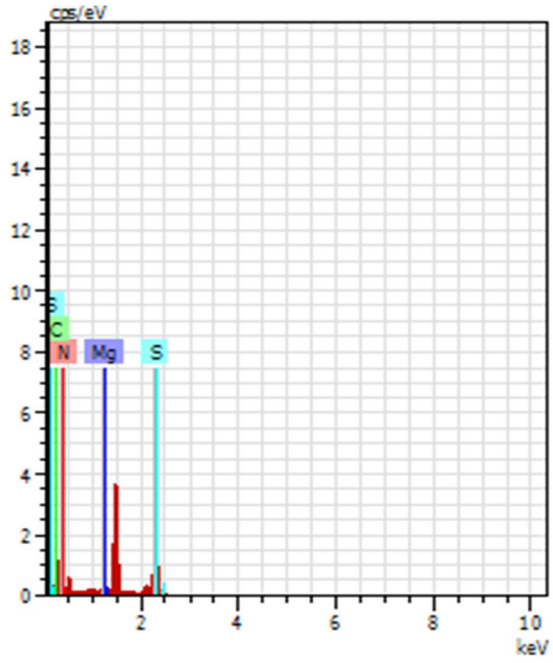

FIG. 6(b) EDAX spectrum of $MgSO_4$-doped TU crystals.

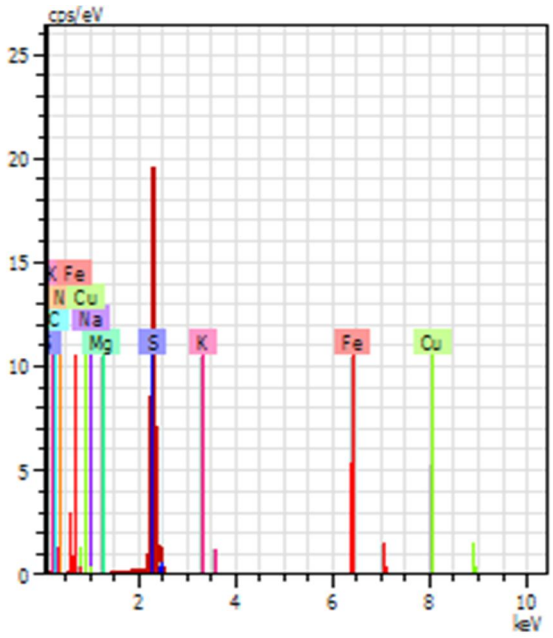

FIG. 6(c) EDAX spectrum of metal complexes of $MgSO_4$-doped TU crystals.

TABLE 4. EDAX data of pure and $MgSO_4$-doped TU and its metal complexes.

Elements	Pure TU		$MgSO_4$-doped TU		Metal complex of $MgSO_4$-doped TU	
	At.Wt. %	Weight%	At.Wt. %	Weight%	At.Wt. %	Weight%
C	31.21	18.89	36.80	31.61	18.26	9.08
N	33.02	23.31	58.85	58.94	23.97	13.89
S	35.77	57.80	3.39	7.78	57.41	76.18
Mg	-	-	0.96	1.67	0.03	0.03
Cu	-	-	-	-	0.28	0.72
K	-	-	-	-	0.03	0.05
Fe	-	-	-	-	0.02	0.05
Na	-	-	-	-	0.00	0.00

Table 4 shows that in pure TU crystals, only the present elements, such as carbon, nitrogen, and sulfur, were found. But in the $MgSO_4$-doped TU, in addition to the parent elements, magnesium was highly incorporated in the parent element. In the metal complex of $MgSO_4$-doped TU, traces of elements like potassium and iron were found.

3.4. Optical studies

An optical transmission spectrum of $MgSO_4$-doped TU and its metal complex crystals was recorded in the range of 200 to 1200 nm using a Perkin Elmer Lambda 35 UV-Visible spectrometer to assess their suitability for optical applications. The spectra shown in Figs. 7(a), 7(b), and 7(c) indicate that both the pure and $MgSO_4$-doped TU crystals, as well as their metal complexes, exhibit good transmittance across the entire visible region. The UV cut-off wavelength of the pure TU crystal was found to be 376.45 nm, with no significant transmission observed beyond this point up to 1200 nm. For the $MgSO_4$-doped TU and its metal complex crystals, the UV cut-off wavelength was 391.30 nm, and again, no considerable transmission occurred up to 1200 nm. The overlaid UV-Vis spectra demonstrate the optical quality of the grown pure and $MgSO_4$-doped TU crystals, along with their metal complexes.

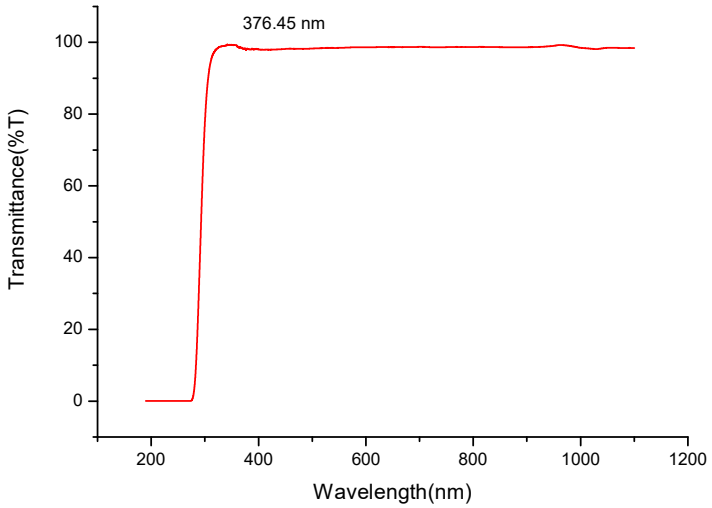

FIG. 7(a) UV transmittance spectrum of pure TU crystal.

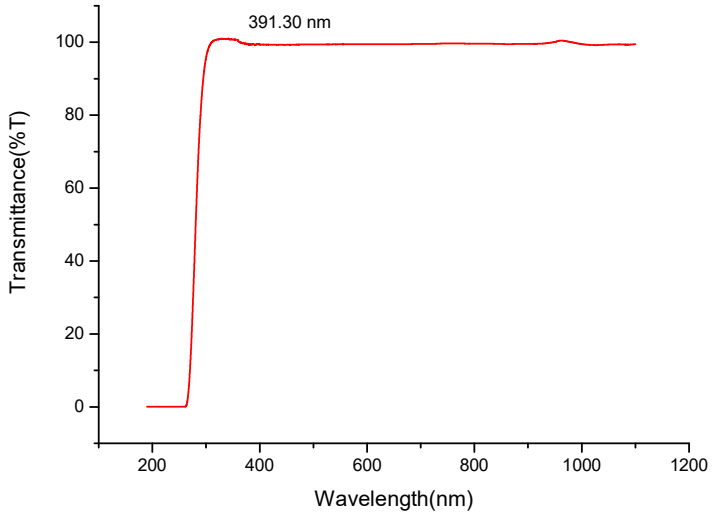

FIG. 7(b) UV transmittance spectrum of $MgSO_4$-doped TU crystals

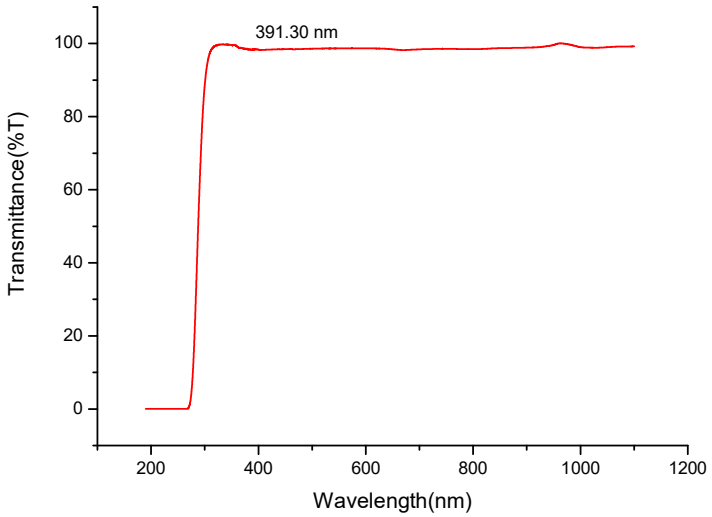

FIG. 7(c) UV transmittance spectrum of metal complex in $MgSO_4$-doped TU crystals.

An optical study shows that the lower cut-off wavelength is 376.45 nm for pure TU crystals. However, the lower cut-off wavelength of the doped TU crystals was found to be enhanced by 14.85 nm, which is 14.85 nm larger than the pure TU.

3.5. Thermal Analysis

Thermogravimetric analysis (TGA) determines decomposition and mass loss over a temperature range. Differential thermal analysis (DTA) determines endothermic and exothermic event temperatures and shows phase transitions. TGA/DTA analysis was done by delicately grinding the TU, $MgSO_4$-doped TU, and metal complexes of MgSO4-doped TU powdered samples to 0.992 mg placed in a crucible deep A1203 pan for STA2500. The thermal stability of the grown crystals of TU, $MgSO_4$-doped TU, and metal complexes of $MgSO_4$-doped TU was analyzed using the NETZSCH STA 2500 at a heating rate of 20°C/min in the temperature range of 30°C to 500°C under a nitrogen atmosphere.

The TGA curve for the grown TU crystal is shown in Fig. 8(a), indicating decomposition and mass changes up to 30°C, with a mass change of -0.91%. The TGA analysis revealed three stages of decomposition. The first stage occurred from 30°C to 100°C, with a mass change of -0.91%. The second stage, from 30°C to 500°C, showed a mass change of -93.76%. The final stage, from 100°C to 500°C, exhibited a mass change of -92.88%. The DTA curve, also shown in Fig. 8(a), reveals three clear endothermic peaks. The first peak started at 180.94°C, the second at 208.44°C, and the third at 458.44°C. These sharp endothermic peaks suggest that the TU crystal has good thermal characteristics.

For the MgSO4-doped TU crystal, the TGA curve in Fig. 8(b) shows decomposition and mass changes up to 30°C, with a mass change of -2.59%. Three stages of decomposition were observed. The first stage, from 30°C to 100°C, had a mass change of -2.59%. The second stage, from 30°C to 495°C, showed a mass change of -99.91%. The final stage, from 100°C to 495°C, exhibited a mass change of -97.32%. The DTA curve in Fig. 8(b) shows three distinct endothermic peaks. The first peak appeared at 181.28°C, the second at 203.78°C, and the third at 411.28°C. The sharpness of these peaks indicates the good nature of the MgSO4-doped TU crystal.

The TGA curve for the MgSO4-doped TU metal complex crystals, shown in Fig. 8(c), shows decomposition and mass changes up to 30°C, with a mass change of -99.58%. Only one stage of decomposition was observed, from 30°C to 222°C, with a mass change of -99.58%. The DTA curve for these crystals, shown in Fig. 8(c), reveals three clear endothermic peaks. The first peak occurred at 80°C, the second at 182.5°C, and the third at 200°C. The sharpness of these peaks indicates that the MgSO4-doped TU metal complex crystal has good thermal stability.

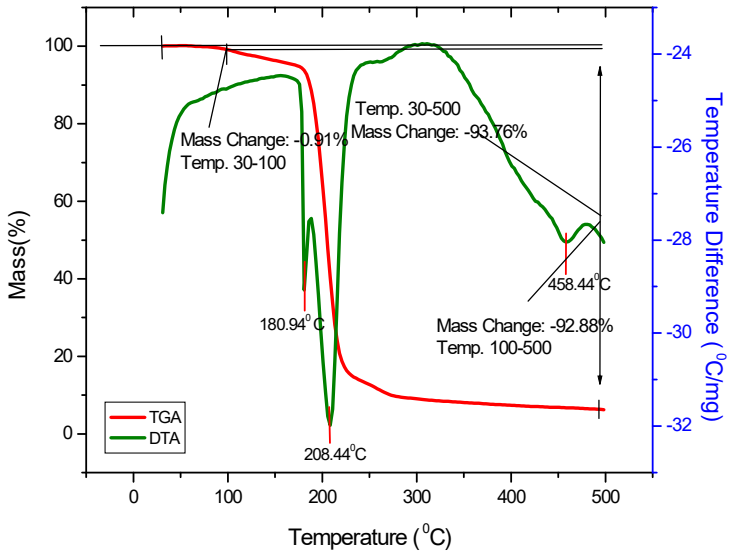

FIG. 8(a) The TGA/DTA curve of the grown TU crystal.

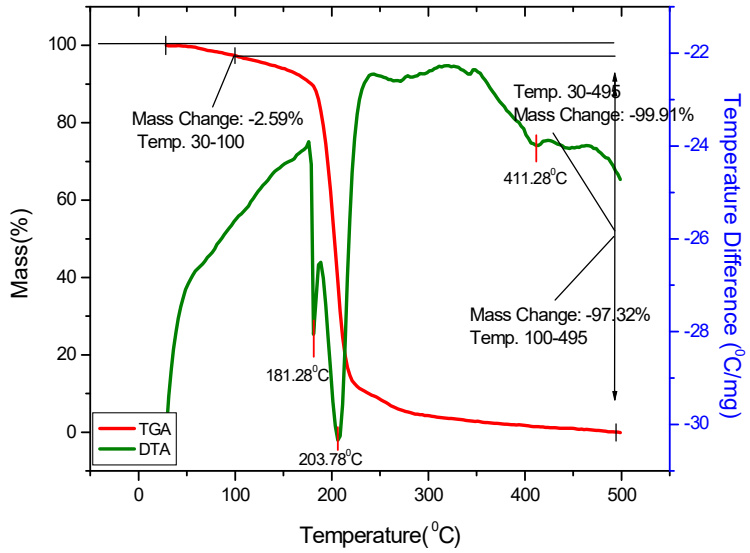

FIG. 8(b) The TGA/DTA curve of the grown $MgSO_4$-doped TU.

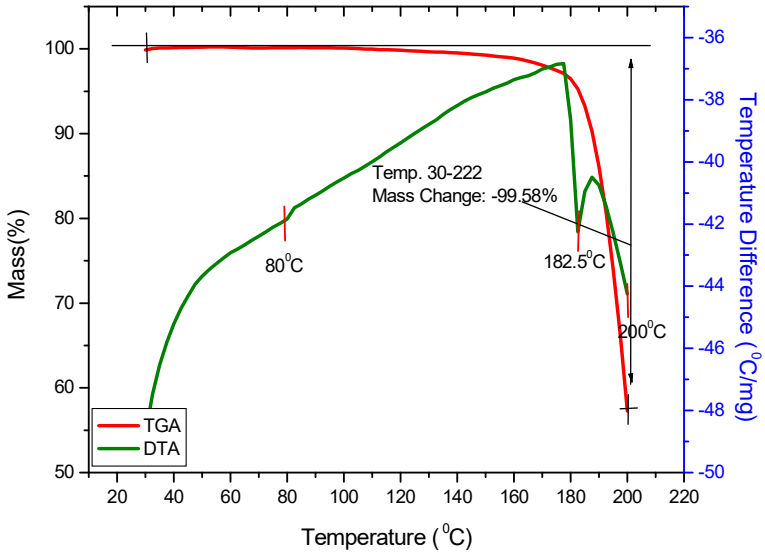

FIG. 8(c) The TGA/DTA curve of the grown $MgSO_4$-doped TU metal complexes.

Conclusion

Pure and $MgSO_4$-doped metal complexes of TU were successfully grown in various dimensions. A change in morphology was observed in the metal complexes of TU. The unit cell volume of the MgSO4-doped crystal showed a slight decrease. The FTIR spectrum of pure, MgSO4-doped, and metal complexes of TU confirmed the incorporation of the dopants. EDXA analysis further validated the formation of a metal complex in TU. UV-visible transmittance measurements indicated an enhancement of 14.85 nm in the lower cut-off wavelength for the metal complex of TU. Thermal studies revealed that the metal complex of TU exhibited good thermal stability.

References

[1] Narayan Bhat, M. and Dharma Prakash, S.M., J. Cryst. Growth, 236 (2002) 376.

[2] Shaked, A., Altaf, A., Qureshi, A.M., and Badshah, A., J. Drug Design Med. Chem., 2 (1) (2016) 10.

[3] El-Bahy, G.M.S., El-Sayed, B.A., and Shabana, A.A., Vib. Spectrosc., 31 (2003) 101.

[4] Kumari, R.G., Ramakrishnan, V., Carolin, M.L., Kumar, J., Sarua, A., and Kuball, M., Spectrochim. Acta A, 73 (2) (2009) 263.

[5] Fleck, M. and Petrosyan, A.M., J. Cryst. Growth, 312 (2010) 2284.

[6] Puzzarini, C., J. Phys. Chem. A, 116 (17) (2012) 4381.

[7] Anie Roshan, A., Joseph, C., and Ittyachen, M.A., Mater. Lett., 49 (2001) 299.

[8] Sanwal, K., Proc. Cryst. Growth, 19 (1989) 189.

[9] Hendricks, S.B., J. Am. Chem. Soc., 50 (1928) 2455.

[10] Selvakumar, S., Packiam Julius, J., Rajasekar, S.A., Ramanand, A., and Sagayaraj, P., Mater. Chem. Phys., 93 (2005) 356.

[11] Selvakumar, S., Rajarajan, K., Ravikumar, S.M., Vetha Potheher, I., Prem Anand, D., and Sagayaraj, P., Cryst. Res. Technol., 41 (2006) 766.

[12] Rajesh, N.P., Kannan, V., Ashok, M., Sivaji, K., Santhana Raaghavan, P., and Ramasamy, P., J. Cryst. Growth, 262 (2004) 561.

[13] Venkataraman, V., Dhanaraj, G., Wadhawan, V.K., Sherwood J.N., and Bhat, H.L., J. Cryst. Growth, 154 (1995) 92.

[14] Ambujam, K., Thomas, P.C., Aruna, S., Prem Anand, D., and Sagayaraj, P., Cryst. Res. Technol., 41 (2006) 1082.

[15] Sivasankaran, S., Illangovan, S., and Arivoli, S., Int. J. Eng. Sci. Invention, 6 (10) (2017) 05.

[16] Kannan, B., Seshadri, P.R., Illangovan, K., and Murugakoothan, P., Indian J. Sci. Technol., 6 (7) (2013) 4909.

[17] Santhi, G. and Alagar, M., Imperial J. Interdiscip. Res. (IJIR), 2 (1) (2016) 537.

[18] Kalaivani, R., Darlin Mary, A., Minisha, S., and Johnson, J., Int. J. Res. Anal. Rev., (IJRAR), 7 (1) (2020) 997.

[19] Jean Mohan Dass, P.N., Umarani, P.R., Victor Antony Raj, M., and Madhavan, J., Der. Pharma. Chem., 5 (4) (2013) 262.

[20] Smith, B.C., "Infrared Spectral Interpretation: A Systematic Approach/ Brain C, Smith". (CRC Press LLC, Boca Raton London New York Washington D.C, 1998) 1-265.

[21]. Zheng, Z.P. and Fan, W.H., J. Biol. Phys., 38 (3) (2012) 405.